

Deformation behavior of SiC particle reinforced Al matrix composites based on EMA model

CHENG Nan-pu(程南璞)^{1,2}, ZENG Su-min(曾苏民)^{1,2,3},
YU Wen-bin(于文斌)^{1,2}, LIU Zhi-yi(刘志义)¹, CHEN Zhi-qian(陈志谦)²

1. School of Materials Science and Engineering, Central South University, Changsha 410083, China;
2. School of Materials Science and Engineering, Southwest University, Chongqing 400715, China;
3. Southwest Aluminium Plant, Chongqing 401326, China

Received 28 March 2006; accepted 12 October 2006

Abstract: Effects of the matrix properties, particle size distribution and interfacial matrix failure on the elastoplastic deformation behavior in Al matrix composites reinforced by SiC particles with an average size of 5 μm and volume fraction of 12% were quantitatively calculated by using the expanded effective assumption(EMA) model. The particle size distribution naturally brings about the variation of matrix properties and the interfacial matrix failure due to the presence of SiC particles. The theoretical results coincide well with those of the experiment. The current research indicates that the load transfer between matrix and reinforcements, grain refinement in matrix, and enhanced dislocation density originated from the thermal mismatch between SiC particles and Al matrix increase the flow stress of the composites, but the interfacial matrix failure is opposite. It also proves that the load transfer, grain refinement and dislocation strengthening are the main strengthening mechanisms, and the interfacial matrix failure and ductile fracture of matrix are the dominating fracture modes in the composites. The mechanical properties of the composites strongly depend on the metal matrix.

Key words: SiC_p/Al composites; deformation behavior; EMA model

1 Introduction

Metal matrix composites reinforced by ceramic particles, with low density, high strength and modulus and flexible fabricating techniques, have received particular attention in the past decades[1]. Some experimental researches have revealed that the macroscopic behavior of this sort of composites depends on the reinforcements (with different volume fraction, particle size and shape), the matrix properties and the metal/particle interfaces. Meanwhile, the particular preparation techniques of the composites rely on these factors[2–5]. In order to describe the effects of such factors on the deformation behavior of the particle reinforced metal matrix composites(PRMMC), the common methods, i.e. the dislocation plasticity theory and the continuum plasticity combined with

Eshelby-inclusion approaches or finite element methods, are often adopted[6–10]. The former theory is successful in describing the deformation behavior of metal matrix composites reinforced by sub-micron particles with a small volume fraction, while the latter is perfect for large reinforcements ($> 10 \mu\text{m}$). However, neither can properly explain the case of reinforcement size between 0.1 and 10 μm . STROUD[11] proposed the effective medium assumption (EMA) model, which can fully cover the range of the reinforcement sizes and bring the dislocation plasticity theory and the continuum plasticity into this model naturally. NAN and CLARKE[12] modified this model to describe the effects of the particle size, shape and fracture on the deformation behavior of PRMMC.

In this paper, by considering the effects of particle size, particle size distribution, microstructure variety of metal matrix and interfacial matrix failure, the EMA

model will be further expanded to calculate the stress-strain correlation of 12%SiC (5μm)/Al composites (volume fraction). The aim of the theoretical results compared with those of our experiment is to investigate the elastoplastic deformation behavior of PRMMC. The strengthening mechanism and the fracture modes of PRMMC were also discussed.

2 Experimental materials and deformation behavior

The metal matrix materials in the composites were atomized powders, whose nominal compositions were (mass fraction, %): Al-1.4Mg-1.22Si-1.19Cu-0.92Mn-0.5Fe, and the reinforcements were horny α-SiC particles. The SiC particle size distribution is usually expressed by a lognormal distribution function, i.e.

$$p(d) = \frac{1}{2\sqrt{\pi}\delta d} \exp\left[-\left(\frac{\ln(d/\bar{d})}{2\delta}\right)^2\right] \quad (1)$$

By fitting Eqn.(1) to the SiC particle size distribution, we got the mean particle size $\bar{d} = 5 \mu\text{m}$ and the standard deviation $\delta = 0.15$, as shown in Fig.1.

The SiC_p/Al composites were fabricated by a powder metallurgy and hot extrusion route. For com-

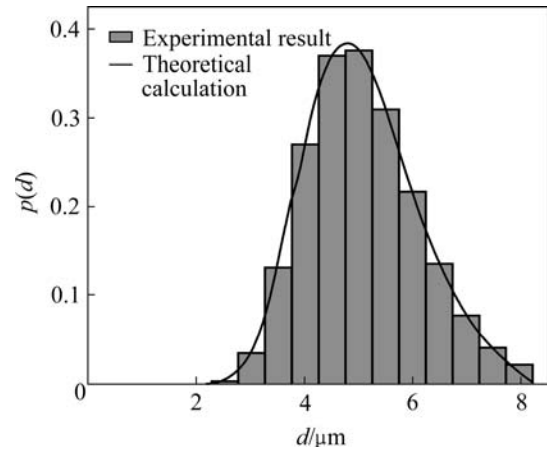


Fig.1 Distribution of SiC particle size

paring experimental and theoretical calculation, the unstrengthened alloy materials were also prepared by the same method. The as-received materials were conducted to T6 heat treatment (solution treated for 60 min at 530 °C, water quenched at 20 °C and aged for 8 h at 170 °C). The tensile properties of the materials were measured on a SUN 5 testing machine.

The metallograph, fracture surface and stress-strain correlation of the materials are shown in Fig.2. In Fig.2(a), the grain size of matrix in composites is small

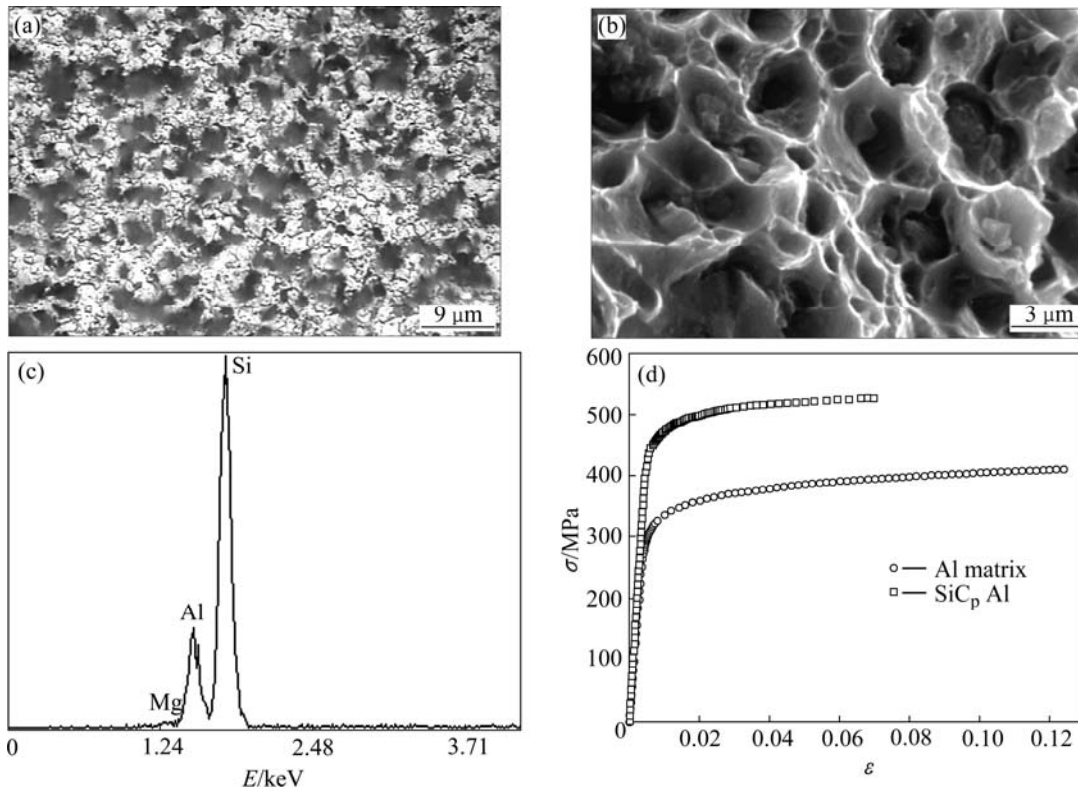


Fig.2 Microstructures and deformation behavior of composites: (a) Metallograph of SiC_p/Al composite; (b) Fracture surface of SiC_p/Al composite; (c) EDX spectrum of SiC particle surface; (d) Stress—strain curves of Al alloy and SiC_p/Al composite during tensile tests

and comparative to the average particle size. The fracture surface (see Fig.2(b)) of the composites and EDX spectrum analysis in Fig.2(c), reveal that the interfacial matrix failure (crack propagation in the near vicinity of the SiC/Al matrix interface) and the ductile fracture of Al matrix are the dominating fracture modes in the composites. The fracture of SiC particles isn't observed, but a few clustered particles are found on the fracture surface. In Fig.2(d), the experimental results show that the elastic modulus, yield strength and fracture strength of the composites are higher than those of the matrix alloy, while the ductility decreases roughly by 50%.

3 EMA model[11–13]

Supposing that the reinforcement is elastic and perfectly bonded to the elastoplastic metal matrix. Both of the non-linear stress-strain correlations of the matrix alloy and the PRMMC can be described by a formula as

$$\sigma = C(\varepsilon) \cdot \varepsilon \quad (2)$$

where the elastoplastic secant stiffness tensor $C(\varepsilon)$ is a function of the instantaneous strain ε . Then the effective secant stiffness C^* of the PRMMC can be defined by

$$\bar{\sigma} = C^*(\bar{\varepsilon}) \cdot \bar{\varepsilon} \quad (3)$$

where $\bar{\varepsilon}$ and $\bar{\sigma}$ are the average strain and stress, respectively.

For convenience in calculation, we separated $C(\varepsilon)$ into two parts as

$$C(\varepsilon) = C^0(\varepsilon^0) + C'(\varepsilon) \quad (4)$$

where $C^0(\varepsilon^0)$ is the effective secant modulus of the homogeneous reference medium and only depends on the homogeneous strain field ε^0 , and $C'(\varepsilon)$ is the instantaneous variation from $C^0(\varepsilon^0)$.

To calculate the deformation behavior of the PRMMC, the metal matrix is thought of the homogeneous reference materials, namely $C^0 = C^m$. Taking k^C and μ^C as the secant bulk and shear moduli of the PRMMC, k^P and μ^P as the elastic bulk and shear moduli of the particles, and k^m and μ^{ms} as the secant bulk and shear moduli of the metal matrix, respectively, the moduli of the PRMMC can be obtained from Eqn.(7) as[13]

$$\begin{cases} \frac{k^C - k^m}{3k^C + 4\mu^{ms}} = V^P \frac{k^P - k^m}{3k^P + 4\mu^{ms}} \\ \frac{\mu^C - \mu^{ms}}{\mu^C + y^s} = V^P \frac{\mu^P - \mu^{ms}}{\mu^P + y^s} \end{cases} \quad (5)$$

where $y^s = \frac{\mu^{ms}(9k^m + 8\mu^{ms})}{6(k^m + 2\mu^{ms})}$ and V^P is the volume

fraction of reinforcements. The assumption of plastic incompressibility for the matrix materials leads to $k^{ms} = k^m$. The particles were considered to be spherical for convenience in the calculation of Eqn.(5).

By splitting the stress and strain tensors into hydrostatic (σ_{kk} and ε_{kk}) and deviatoric (σ'_{ij} and ε'_{ij}) parts, their components from Eqn.(4) are written as

$$\begin{cases} \bar{\varepsilon}_{kk} = \frac{3k^m + 4\mu^{ms}}{3k^C + 4\mu^{ms}} \varepsilon_{kk}^m, & \bar{\sigma}_{kk} = \frac{3k^m + 4\mu^{ms}}{3k^C + 4\mu^{ms}} \frac{k^C}{k^m} \sigma_{kk}^m \\ \bar{\varepsilon}'_{ij} = \frac{\mu^{ms} + y^s}{\mu^C + y^s} \varepsilon'_{ij}{}^m, & \bar{\sigma}'_{ij} = \frac{\mu^{ms} + y^s}{\mu^C + y^s} \frac{1}{\mu^{ms} \mu^C} \sigma'_{ij}{}^m \end{cases} \quad (6)$$

and the stress components in particles are

$$\begin{cases} \sigma_{kk}^P = \frac{3k^m + 4\mu^{ms}}{3k^C + 4\mu^{ms}} \frac{k^P}{k^m} \sigma_{kk}^m \\ \sigma'_{ij}{}^P = \frac{\mu^{ms} + y^s}{\mu^C + y^s} \frac{\mu^P}{\mu^{ms}} \sigma'_{ij}{}^m \end{cases} \quad (7)$$

The empirical Ramburg-Osgood equation(ROE) is reasonable and often used to describe the uniaxial stress-strain behavior for the metal materials, namely

$$\varepsilon^m = \frac{\sigma^m}{E^m} + \alpha \frac{\sigma_Y^m}{E^m} \left(\frac{\sigma^m}{\sigma_Y^m} \right)^{1/n} \quad (8)$$

where E^m , σ_Y^m and n are the elastic modulus, yield strength and strain working exponent of the matrix, respectively and α is a constant. After measuring the stress—strain curve of the matrix materials, σ_Y^m , α and n can be got by fitting the experimental results in Fig.2(c) through Eqn.(8). Then the secant elastic modulus of the matrix metal materials is represented by

$$E^{ms} = \frac{E^m}{1 + \alpha \left(\frac{\sigma_{11}^m}{\sigma_Y^m} \right)^{\frac{1-n}{n}}} \quad (9)$$

and the secant shear modulus, under the condition of plastic incompressibility during deformation, is written as

$$\mu^{ms} = \frac{E^{ms}}{3 - E^{ms} / 3k^m} \quad (10)$$

The secant shear modulus μ^{ms} of the matrix material under the uniaxial tensile load σ_{11} (the effective stress in uniaxial deformation) can be calculated from Eqns.(8)–(10). Substituting its values into Eqn.(6), we get the average stress-strain correlation of the composites and plot it in Fig.3. The parameters for theoretical calculation are summarized in Table 1.

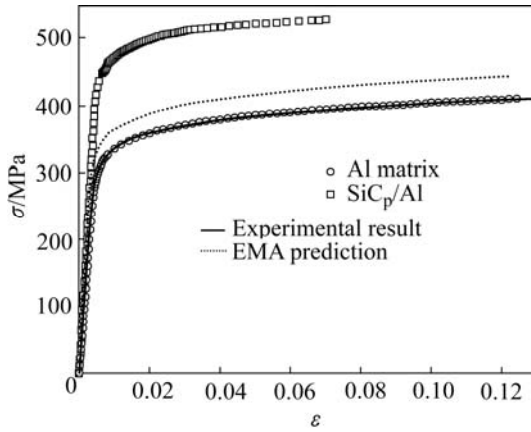


Fig.3 Comparison between EMA prediction and experimental results

Table 1 Properties of SiC and Al matrix materials

| Material | Elastic modulus, E/GPa | Poisson's ratio, ν | Coefficient of thermal expansion/ ($10^{-6}\cdot\text{K}^{-1}$) | |
|--------------|------------------------------------|--|--|-------|
| Al matrix | 69.6 | 0.33 | 23.4 | |
| SiC particle | 450 | 0.17 | 4.3 | |
| Material | Burgers vector/nm | Yield strength, σ_Y^m/MPa | α | n |
| Al matrix | 0.286 | 315 | 0.457 | 0.065 |
| SiC particle | – | – | – | – |

In Fig.3, the calculated elastic modulus of the PRMMC agrees well with that of the experiment. The reinforcements can bear partial load and then enhance the flow stress of the composites (that's to say, the tensile load can transfer between matrix and reinforcements), which can also be derived from Eqn.(6). However, the theoretical results are much lower than those of experiment during the plastic deformation. The reason is that the microstructure variation of matrix, particle size (distribution) and interfacial matrix failure is not taken into account, only the volume fraction of the reinforcements is considered in the simple EMA model. At the same time, this means that the plastic deformation behaviors predicted by the EMA model of PRMMC with different particle sizes are the same, which deviates from the reality. Commonly, with the same volume fraction of

the reinforcements, the smaller the particle size is, the higher the flow stress is in PRMMC.

The grain size of matrix in PRMMC, compared with the monolithic matrix alloy produced by the same process, will be refined much due to the addition of fine and tough particles. This is because that the tough particles can cut the matrix, and at the same time, their presence increases the effective extrusion ratio during the hot extrusion process. The thermal mismatch between particles and metal matrix will bring higher dislocation density into matrix near the particle surfaces during cooling in process, and the sub-grains in matrix formed by the dislocation lines are very small. The Orvan mechanism of the reinforcements will act due to their small size. Meanwhile, the strain gradient effects, associated with geometrically necessary distribution of dislocations(GND) that are required to accommodate the plastic strain mismatch between the particles and the surrounding matrix during tensile deformation, will influence the flow stress. All these factors will certainly enhance the strength of matrix in PRMMC[14–16].

4 Effect of reinforcements on matrix

For very small reinforcement, the Orvan mechanism likely acts and reads[17]

$$\Delta\sigma_{or}^m = 2\mu^m b / (\pi d^2 / 4V^p)^{1/2} \quad (11)$$

where μ^m and b are the shear modulus, Burgers vector of the matrix materials, and d and V^p are the particle size and volume fraction, respectively.

The contribution of the strain gradient effects to the flow stress during the plastic deformation is represented by[15–16]

$$\Delta\sigma_{gnd}^m = \beta\mu^m \left(\frac{V^p \varepsilon_p b}{d} \right)^{1/2} + \gamma\mu^m V^p \left(\frac{\varepsilon_p b}{d} \right)^{1/2} \quad (12)$$

where $\beta \approx 0.4$ and $\gamma \approx 0.2$ are two geometric constants associated with the particle topology respectively, and ε_p represents the plastic strain.

The effect of the grain refinement of matrix in composites during the hot extrusion on the flow stress can be described by the Hall-Patch correlation[18–19]

$$\Delta\sigma_{ref}^m \approx \lambda D^{-1/2} \approx \lambda d^{-1/2} \left(\frac{1-V^p}{V^p} \right)^{1/6} \quad (13)$$

where $\lambda \approx 0.1 \text{ MPa} \cdot \text{m}^{1/2}$ is a strengthening factor.

The high-density dislocations stemmed from processing and thermal expansion mismatch on cooling

(such as water quenching) will strengthen the composites, which can be expressed by[12, 17]

$$\Delta\sigma_{cte}^m = \eta\mu^m b\sqrt{\Delta\rho} = \eta\mu^m b\sqrt{\frac{6|\Delta T\Delta\alpha|V^P}{bd(1-V^P)}} \quad (14)$$

where $\eta \approx 2.7$ is a constant (same as Ref.[12]), $\Delta\alpha$ is the difference of thermal expansion mismatch and ΔT is the difference in temperature from heat treatment temperature of matrix to room temperature.

The contributions described by Eqns.(11)–(14) are eventually ascribed to the addition of SiC particles into the metal matrix. Due to the presence of the SiC particles, the total strengthening effects $\Delta\sigma^m$ can be chosen as[20]

$$\Delta\sigma^m = \sqrt{(\Delta\sigma_{or}^m)^2 + (\Delta\sigma_{gnd}^m)^2 + (\Delta\sigma_{ref}^m)^2 + (\Delta\sigma_{cte}^m)^2} \quad (15)$$

then the original yield stress σ_Y^m of ROE in Eqn.(1) will be replaced by

$$\sigma_Y^{m*} = \sigma_Y^m + \Delta\sigma^m \quad (16)$$

Noting that the particle size d is variable (see Fig.1 and Eqn.(1)), the particle size distribution should be considered in calculating Eqns.(11)–(14), namely

$$\sigma_Y^{m*} = \sigma_Y^m + \langle \Delta\sigma^m \rangle = \sigma_Y^m + \int p(d)\Delta\sigma^m dd$$

and the theoretical result is plotted in Fig.4.

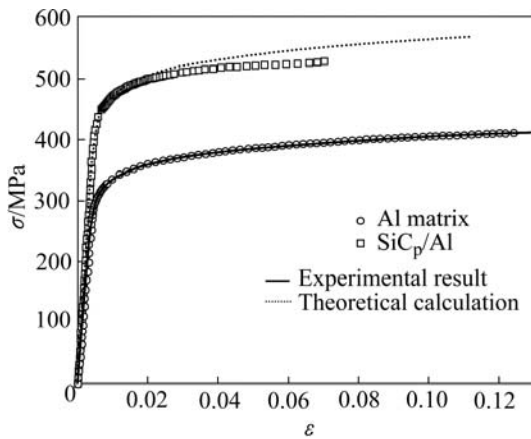


Fig.4 Comparison between theoretical calculation and experimental results after considering size distribution of SiC particles and their effects on Al matrix

In Fig.4, when the effects of the Orwan mechanism, the strain gradient plasticity, the grain refinement of matrix and the high dislocation density due to thermal expansion mismatch are taken into account, the calculated stress—strain curve of the composites is consistent with the experimental results in the low strain

region ($\varepsilon < 2\%$). However, the theoretical results are higher than those of experiment in the large strain region ($\varepsilon > 2\%$). This is because that the particles are assumed to be perfectly bonded with the metal matrix, which is untenable in the large strain region due to the interfacial matrix failure up to rupture of the composites (see Fig.2(b)).

5 Effect of interfacial matrix failure on deformation

Studies on the fracture mechanism of PRMMC indicate that the particle fracture dominates a rupture of the composites reinforced by large particles (e.g., $d > 20 \mu\text{m}$), while the interfacial debonding plays a critical role in the case of small reinforcements (e.g., $d < 10 \mu\text{m}$) [21–25]. The average size of the reinforcement particles is $5 \mu\text{m}$ ($d_{\text{max}} < 8.5 \mu\text{m}$) in our experiment. From Figs.2(b) and (c), we know that the fracture of the composites mainly contains the interfacial matrix failure and the ductile fracture of metal matrix. The interfacial matrix failure observed in the composites is different from the simple interfacial debonding that the SiC particles are pulled out from metal matrix with clear surfaces[25]. There exist two concepts about the interfacial rupture of PRMMC, i.e. the cohesive energy ϕ_{coh} and the cohesive strength σ_{coh} . When the strain energy (or the stress strength) of the observed interfaces between particles and matrix is equal to or greater than the corresponding cohesive energy (or the cohesive strength), the interfacial failure will take place during the tensile deformation[26–28]. The research on the cohesive zone model of PRMMC reveals that ϕ_{coh} has a large variation from J/m^2 to kJ/m^2 and σ_{coh} from MPa to GPa. It is difficult to determine their values in theory, and there are no available data about the cohesive energy or the cohesive strength for the interfaces between Al matrix and SiC particles. Based on LLOYD's work[28], the large particles in composites will easily break due to their low fracture strength varying directly as $1/\sqrt{d}$, where d is the particle size. The viewpoint of the cohesive strength that is supposed to comply with the same particle size dependence as LLOYD's result, namely $\sigma_{\text{coh}} \propto 1/\sqrt{d}$, is adopted in this paper. By fitting the experimental results in Fig.2(d), we can simply determine the average cohesive strength $\sigma_{\text{coh}} \approx 530 \text{ MPa}$. When the particle size distribution is taken into account, the cohesive strength for different particle sizes will be rewritten as $\sigma_{\text{coh}}(d) \approx 1185 \text{ MPa} \cdot \mu\text{m}^{1/2}/\sqrt{d}$, where the unit of d is micron. If the effective interfacial stress of a particle with size d reaches the corresponding interfacial cohesive strength $\sigma_{\text{coh}}(d)$ during the tensile deformation, the observed interface begins to fail, and the particle is treated as a hole and the total volume

fraction of particles in the composites reduces. Measuring the interfacial stress is a difficult work, so a simple hypothesis similar to Eqn.(15) was utilized to characterize the effective interfacial stress for the corresponding strain by

$$\sigma_e^{\text{int}} = \sqrt{\left(\sigma_e^{\text{m}}\right)^2 + \left(\sigma_e^{\text{p}}\right)^2} / 2 \quad (17)$$

where σ_e^{m} and σ_e^{p} are the effective stresses of matrix and particles respectively, which can be obtained from Eqns.(6) and (7). The calculated stress—strain curve of the composites, after considering the effect of interfacial matrix failure, is shown in Fig.5. This reveals that the theoretical flow stress compared with that of Fig.4 decreases, and is a little higher than experimental results in the large strain region. The probable reason for the disparity is that the effects of clustered particles, existing in the composites and without strengthening effects, were not considered in the theoretical calculation.

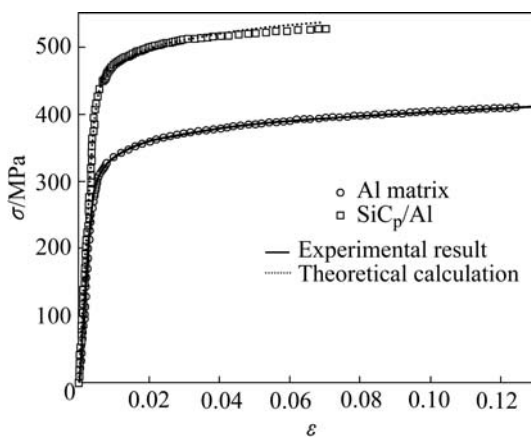


Fig.5 Effects of interfacial matrix failure on deformation in SiC_p/Al composites

6 Analysis and results

By only considering the effects of volume fraction of particles and the load transfer, the simple EMA model (not expanded) neither reasonably explains the deformation behavior of PRMMC nor reflects the effects of microstructure variation of matrix, particle size distribution and interfacial failure. When the microstructure variation of matrix in composites due to the presence of SiC particles is taken into account, the theoretical flow stress coincides well with the experimental one in low strain region. By numerically estimating through Eqn.(6), the load transfer mechanism devotes roughly 30 MPa to the strength of the composites. From Eqns.(11)–(14) we know that both of the average contributions of the Orwan theory and the strain gradient effect on the strength are less than 10 MPa, while those of the grain refinement of matrix and

the high dislocation density as a result of the thermal mismatch are close to 60 MPa. This means that the dislocation strengthening, crystalline refinement and load transfer are the major strengthening mechanism of the PRMMC produced in our experiment.

When the interfacial matrix failure is considered, the theoretical results in large strain region decrease and coincide well with experimental results. The particle size distribution is simultaneously embodied in the microstructure variation of matrix and the interfacial matrix failure. Particularly, the interfaces of the larger particles prior to the smaller ones are easy to rupture because of their relatively low cohesive strength. The interfaces of the smaller particles are likely to fail with the further increase of the effective interfacial stress during the tensile deformation. If the effective interfacial stress of the very small particles cannot reach the corresponding cohesive strength, the interfaces will not fail and the crack only proceeds in metal matrix. According to the viewpoint of particle fracture, when the effective stress inside the SiC particles comes up to $2\ 500\text{--}3\ 000\ \text{MPa}\cdot\mu\text{m}^{1/2}/\sqrt{d}$ during deformation, the SiC particles will break. The fracture strength of the SiC particles used in our experiment is about 858–1 029 MPa that is larger than the theoretical value from Eqn.(7), so all the SiC particles will not rupture. The fracture surface in Fig.2(b) gives an evidence that there is no SiC particle rupture in the composites. Hence, the interfacial matrix failure and the ductile fracture of metal matrix are the main fracture modes in these composites.

7 Conclusions

- 1) The expanded EMA model can reasonably explain the uniaxial deformation behavior of the Al matrix composites reinforced by SiC particles with an average size of 5 μm and volume fraction of 12%.
- 2) Through the comparison between the theoretical calculation and experimental results, the load transfer, the grain refinement and the high dislocation density will enhance the flow stress of the metal matrix composites reinforced by micro-scale SiC particles, and that they are the major strengthening mechanisms of the PRMMC.
- 3) The gradual interfacial matrix failure of SiC particles will reduce the flow stress of the composites during tensile deformation. The interfacial matrix failure and the ductile fracture of metal matrix are the main fracture modes, and the deformation behavior of the composites strongly depends on the properties of matrix.

Acknowledgement

The authors CHENG and ZENG to Professors LI

Wen-xian and WANG Ri-chu for their supplying the raw materials in experiment.

References

- [1] DIVECHA A P, FISHMAN S G, KARMARKAR S D. Silicon carbide reinforced aluminum—A formable composite [J]. *J Metals*, 1981, 33(9): 12–17.
- [2] FAN Jian-zhong, SHANG Ji-mei. The spatial distribution of reinforcements in aluminum matrix composites [J]. *Acta Metall Sinica*, 1998, 34(11): 1199–1204. (in Chinese)
- [3] HU Geng-kai, HAN Qi. Influence of inclusion's orientation and spatial distribution on elastic-plastic properties of composites [J]. *J Beijing Inst Technol*, 1999, 19(5): 554–559. (in Chinese)
- [4] LÜ Yu-xiong, BI Jing, CHEN Li-qing, ZHAO Ming-jiu. Effects of particle size and matrix strength on the failure mechanism of SiC_p reinforced aluminium matrix composites [J]. *Acta Metall Sinica*, 1998, 34(11): 1188–1192. (in Chinese)
- [5] XIAO Bo-lü, BI Jing, ZHAO Ming-jiu, MA Zhong-yi. Effects of SiC_p size on tensile property of aluminum matrix composites fabricated by powder metallurgical method [J]. *Acta Metall Sinica*, 2002, 38(9): 1006–1008. (in Chinese)
- [6] HUMPHREYS F J. *Dislocations and Properties of Real Materials* [M]. London: Inst of Metals, 1985: 175.
- [7] FAN Jian-hua, XU Qing-yu. Equivalent differential computation on modulus of composites [J]. *J Eng Math*, 2003, 20(1): 93–98. (in Chinese)
- [8] FANG Dai-ning, ZHOU Chu-wei. Numerical analysis of the mechanics behavior of composites by finite element micromechanic method [J]. *Adv Mech*, 1998, 28(2): 173–188. (in Chinese)
- [9] LIANG Jun, DU Shan-yi. Study of the mechanical behavior of the elastoplastic matrix composites by micromechanics [J]. *Acta Mechanica Solida Sinica*, 2000, 21(4): 361–365. (in Chinese)
- [10] MISHNAEVSKY JR L, DONG M, HÖNLE S, SCHMAUDER S. Computational mesomechanics of particle-reinforced composites [J]. *Comput Mater Sci*, 1999, 16: 133–143.
- [11] STROUND D. The effective medium approximations: Some recent developments [J]. *Superlattices Microstruct*, 1998, 23(3/4): 567–573.
- [12] NAN C W, CLARKE D R. The influence of particle size and particle fracture on the elastic/plastic deformation of metal matrix composites [J]. *Acta Mater*, 1996, 44: 3801–3811.
- [13] HU G K, GAO G, BAPTISE. A micromechanical model of influence of particle fracture and particle cluster on mechanical properties of metal matrix composites [J]. *Comput Mater Sci*, 1998, 9: 420–430.
- [14] YU Yong-ning, FANG Zhi-gang. An introduction to metal matrix composites [M]. Beijing: Metallurgical Industry Press, 1996: 79–81. (in Chinese)
- [15] XUE Z, HUANG Y, LI M. Particle size effect in metallic materials: a study by the theory of mechanism-based strain gradient plasticity [J]. *Acta Mater*, 2002, 50: 149–160.
- [16] GAO H, HUANG Y, NIX W D, HUTCHINSON J W. Mechanism-based strain gradient plasticity (I): Theory [J]. *J Mech Phys Solids*, 1999, 47: 1239–1263.
- [17] ARSENAULT R J, SHI N. Dislocation generation due to difference between coefficients of thermal expansion [J]. *Mater Sci Eng A*, 1986, A81: 175–178.
- [18] HALL E O. The deformation and ageing of mild steel (III) [J]. *Proc Phys Soc*, 1951, B64: 747–753.
- [19] PETCH N J. The cleavage strength of polycrystals [J]. *J Iron Steel Inst*, 1953, 174: 25–28.
- [20] CLYNE T W, WITHERS P J. *An Introduction to Metal Matrix Composites* [M]. Cambridge: Cambridge University Press, 1993.
- [21] CHEN Z Z, TOKAJI K. Effects of particle size on fatigue crack initiation and small crack growth in SiC particulate-reinforced aluminium alloy composites [J]. *Mater Lett*, 2004, 58: 2314–2321.
- [22] SHYONG J H, DERBY B. The deformation characteristics of SiC particulate-reinforced aluminium alloy 6061 [J]. *Mater Sci Eng A*, 1995, A197: 11–18.
- [23] KAPOOR R, VECCHIO K S. Deformation behavior and failure mechanisms in particulate reinforced 6061 Al metal-matrix composites [J]. *Mater Sci Eng A*, 1995, A202: 63–75.
- [24] GUPTA M, SURAPPA M K, QIN S. Effect of interfacial characteristics on the failure-mechanism mode of a SiC reinforced Al based metal-matrix composite [J]. *J Mater Process Technol*, 1997, 67: 94–99.
- [25] NIE S H, BASARAN C. A micromechanical model for effective elastic properties of particulate composites with imperfect interfacial bonds [J]. *Int J Solids Struct*, 2005, 42: 4179–4191.
- [26] JIAO S, JENKINS M L, DAVIDGE R W. Interfacial fracture energy-mechanical behavior relationship in Al₂O₃/SiC and Al₂O₃/TiN nanocomposites [J]. *Acta Mater*, 1997, 45(1): 149–156.
- [27] CHANDRA N, LI H, SHET C, GHONEM H. Some issues in the application of cohesive zone models for metal-ceramic interfaces [J]. *Int J Solids Struct*, 2002, 39: 2827–2855.
- [28] LLOYD D J. Particle reinforced aluminum and magnesium matrix composites [J]. *Int Mater Rev*, 1994, 39: 1–23.

(Edited by LI Xiang-qun)